HHS Public Access

Author manuscript

J Tissue Eng Regen Med. Author manuscript; available in PMC 2020 March 27.

Published in final edited form as:

J Tissue Eng Regen Med. 2019 September ; 13(9): 1724–1731. doi:10.1002/term.2924.

Kidney-in-a-lymph node: A novel organogenesis assay to model human renal development and test nephron progenitor cell fates

Maria Giovanna Francipane[1,2], **Bing Han**[1], **Leif Oxburgh**[3], **Sunder Sims-Lucas**[4], **Zhongwei Li**[5], **Eric Lagasse**[1]

[1]McGowan Institute for Regenerative Medicine and Pathology Department, University of Pittsburgh, Pittsburgh, Pennsylvania

[2]Ri.MED Foundation, Palermo, Italy

[3]Center for Molecular Medicine, Maine Medical Center Research Institute, Scarborough, Maine

[4]Rangos Research Center, Children's Hospital of Pittsburgh of UPMC, Pittsburgh, Pennsylvania

[5]Department of Stem Cell Biology and Regenerative Medicine, Keck School of Medicine of USC, Los Angeles, California, USA

Abstract

Stem cell-derived organoids are emerging as sophisticated models for studying development and disease and as potential sources for developing organ substitutes. Unfortunately, although organoids containing renal structures have been generated from mouse and human pluripotent stem cells, there are still critical unanswered questions that are difficult to attain via in vitro systems, including whether these nonvascularized organoids have a stable and physiologically relevant phenotype or whether a suitable transplantation site for long-term in vivo studies can be identified. Even orthotopic engraftment of organoid cultures in the adult does not provide an environment conducive to vascularization and functional differentiation. Previously, we showed that the lymph node offers an alternative transplantation site where mouse metanephroi can differentiate into mature renal structures with excretory, homeostatic, and endocrine functions. Here, we show that the lymph node lends itself well as a niche to also grow human primary kidney rudiments and can additionally be viewed as a platform to interrogate emerging renal organoid cultures. Our study has a wide-ranging impact for tissue engineering approaches to rebuild functional tissues in vivo including—but not limited to—the kidney.

Keywords

bioreactor; functional maturation; kidney engineering; kidney organogenesis; lymph node; nephron progenitors

Correspondence Maria Giovanna Francipane, PhD, McGowan Institute for Regenerative Medicine and Pathology Department, University of Pittsburgh, Bridgeside Point II. 450 Technology Drive, Suite 333, Pittsburgh, PA 15219., mariagiovannafrancipane@gmail.com.

CONFLICT OF INTEREST

Eric Lagasse is the scientific founder and the Chief Scientific Officer of LyGenesis, Inc.

SUPPORTING INFORMATION

Additional supporting information may be found online in the Supporting Information section at the end of the article.

1 | OVERVIEW

Recent discoveries about how cells self-organize are driving the creation of organ models for research or transplantation. Different artificial means, such as matrix molecules, silk films, and chips, among others, are being exploited to generate three-dimensional structures from tissue-specific stem cells, embryonic stem cells, and induced pluripotent stem cells (Francipane & Lagasse, 2016b). These culture systems allow the researcher to address specific questions concerning how the intricate processes of development, homeostasis, and disease unfold and open up new avenues for regenerative medicine as well as disease correction (Xu et al., 2018).

In the context of kidney, the metanephric organ culture—used for decades to unveil the cellular and molecular interplay associated with nephrogenesis (Grobstein & Dalton, 1957)—has made room for organoid cultures from lineage-specified progenitors (Taguchi et al., 2014). Valuable aspects of nephrogenesis and pathogenesis of renal diseases have been recapitulated in vitro using these methods (Freedman et al., 2015; Takasato et al., 2015). However, animal transplantation is often needed to supply organoid cultures with a vascular system and obtain fully mature nephrons to be used in putative medical applications (Hariharan, Kurtz, & Schmidt-Ott, 2015). Renal subcapsular transplantation of kidney organoids has been exploited to induce neo-vasculogenesis (van den Berg et al., 2018), but this approach suffers from poor clinical translatability as the inflammatory and fibrotic milieu of a chronically injured kidney might not support the engraftment, survival, and function of the transplanted cells. In addition, clinical progress in renal subcapsular transplantation has lagged behind other techniques due to the inelastic and tight nature of the human renal subcapsular space (Sakata, Yoshimatsu, & Kodama, 2018).

In our quest to find an ideal site for kidney cell/tissue transplantation, we have found the lymph node (LN) to be a good candidate. LNs are secondary lymphoid organs, in which lymphocytes fight off bacteria, viruses, cancer cells, and nonself substances that have entered the body.

Our prior studies described the LN as an attractive bioreactor supporting the engraftment and function of adult mouse hepatic, pancreatic, and thymic cells (Komori, Boone, DeWard, Hoppo, & Lagasse, 2012) as well as the functional maturation of several mouse embryonic tissues, including the kidney (Francipane & Lagasse, 2014, 2015, 2016a).

Here, we demonstrate that similar to the mouse embryonic kidney, the human fetal kidney engrafts and displays physiological functions inside the LN, thanks to the excellent degree of host-derived vascularization. Finally, we show the potential of using the LN bioreactor to investigate candidate self-organized tissues. By doing so, we propose the LN as a next-generation platform to validate de novo renal progenitor-derived kidney tissues in vivo. Such a platform is vital to identify differentiation protocols that give rise to cells that remain differentiated in vivo and to determine the fate(s) of those cells that do not differentiate and might pose a risk for teratoma development. Also, this platform allows assessment of the potential of vascularized renal organoids to attain physiological functions in vivo.

Human fetal kidneys (between 14 and 23 weeks of gestation) were used as donor tissue for transplantation into the LN. Although there are well-developed glomeruli and tubules at these stages, there is also a nephrogenic zone just underneath the renal capsule containing different progenitor populations (Short et al., 2014). We used this zone to obtain tissue fragments to be transplanted into the jejunal LN (Figure 1a, left panels and Data S5 for detailed information about all procedures). Athymic BALB/c nude mice were chosen as immunodeficient transplant recipients to avoid T cell–mediated rejection (Rygaard & Povlsen, 1969). Three weeks after transplantation, an initial LN examination suggested tissue engraftment and no evidence of rejection (Figure 1a, right panels). A thorough immunohistochemical characterization followed (see Data S6 for information about the antibodies used). Staining of the engrafted LNs for the mouse pan-leukocyte marker CD45 suggested that maturing kidney tissues were devoid of infiltrating immune cells (Figure 1b). Nonhematopoietic host cells were detected inside the grafts (Figure 1c). Distinction between mouse and human cells was achieved by exploiting the differential expression of the major histocompatibility complex antigens. Specifically, we used antibodies for H-2kd and human leukocyte antigen (HLA) to detect host BALB/c nude mouse and donor human cells, respectively. Alternatively, we used an antihuman mitochondria antibody (hMIT) for human cells. Host infiltrating cells were mainly endothelial cells (ECs, CD31 staining, Figure 1d). Intraglomerular mouse vessels were newly formed vessels (CD105 staining) and contained mouse erythrocytes (Ly-76, Figure 1d), indicating blood perfusion. Host EC infiltration occurred as early as 1 week after transplantation, when human donor- and mouse host-derived ECs coexisted (Figure 1e). By the third week, glomeruli were entirely revascularized by mouse ECs, and the caliber of mouse extraglomerular blood vessels reached its maximum level by 8 weeks (Figure 1e).

Additional immunofluorescence stains performed in 3-week grafts indicated normal structures (Figure 1f). We detected neural cell adhesion molecule (NCAM)+ cells in a subset of glomerular cells compatible with parietal epithelial cells. Podocytes were investigated using antibodies against Wilms' tumor 1 (WT-1), Podoplanin (PDPLN), or Podocalyxin (PODXL), and for mesangial cells we used an anti-αsmooth muscle actin (α-SMA) antibody. We observed nuclear to cytoplasmic reactivity for WT-1 in different renal compartments including the vascular pole 3-week posttransplantation, possibly indicating the presence of both WT-1 positive parietal podocytes (Bariety, Mandet, Hill, & Bruneval, 2006) and non–fully differentiated elements (Kreidberg, 2010) at this stage. At later stages of transplantation (8 weeks), WT-1 exclusively localized in the nuclei of intraglomerular cells consistent with podocytes, thus suggesting efficient graft maturation (Figure S1 supporting information). Proximal tubules were analyzed using anti-Megalin (which can also stain podocytes), Aquaporin 1 (AQ1), or Lotus tetragonolobus lectin (LTL) antibodies. Staining for the Sodium-Potassium-Chloride Cotransporter 2 (NKCC2) identified the thick ascending limb of the loop of Henle; NKCC2 expression was compatible with cytoplasmic vesicles in the tubular lumen (Nielsen, Maunsbach, Ecelbarger, & Knepper, 1998). A combination of BRN1 (POU3F3) and Dolichos biflorus agglutinin (DBA) antibodies distinguished loops of Henle (BRN1+/DBA-) from distal tubules (BRN1+/DBA+). Finally, Aquaporin 2 (AQ2) antibody identified the collecting ducts. We next investigated whether such human kidney grafts could have hormonal functions by staining for erythropoietin

(EPO), necessary for erythropoiesis, and Cytochrome P450 Family 27 Subfamily B Member 1 (CYP27-B1, also known as 1alpha-OHase), necessary for the conversion of calcifediol to active calcitriol. EPO is produced primarily by the kidney in response to hypoxia. Specifically, renal peritubular interstitial fibroblast-like cells are the major producers of EPO under this condition (Lacombe et al., 1988; Pan et al., 2011). Moreover, EPO can also be produced under normoxia by intercalated cells of the collecting ducts and proximal and distal tubules (Nagai et al., 2014). Finally, very recent evidence shows the existence of an additional EPO-producing cell population of perivascular stromal cells, which driven by vascular endothelial growth factor A, is capable of increasing EPO production independently from hypoxia (Greenwald et al., 2019). We have never observed interstitial cell production of EPO in our kidney grafts. Rather, our staining pattern is compatible with epithelial EPO production (Figure 1g and Supplementary Figure 2). We also found CYP27-B1 to be expressed in different nephron segments including the proximal tubules (Figure 1g), in accordance with previous studies investigating its distribution in the kidney (Zehnder et al., 1999).

Partial three-dimensional reconstruction from the digital images of hematoxylin and eosin-stained serial sections of an 8-week graft confirmed the presence of glomerular and tubular structures still properly arranged (Stereo Investigator; Figure 1h). Moreover, 10,000 MW Dextran (D1863, Thermo Fisher) uptake in proximal tubules of LN grafts at even later stages (11 weeks) indicated long-term human kidney tubular functions (Figures 1i and S3). The accumulation of Dextran in proximal tubules is likely due to the loss of more distal segments at this stage of engraftment. Indeed, our experience suggests long-term retention of the glomeruli while the renal tubules (especially the distal segments) are progressively lost. This phenomenon is not due to fibrosis or the conversion of the LN into a fibrotic environment, as suggested by staining for Erasmus University Rotterdam-Thymic Reticulum (ER-TR7), CD44, and platelet-derived growth factor receptor beta (PDGFR-β; Figure S4), which are expressed in kidney during development and/or adult life (Crisi, Marconi, Rockwell, Braden, & Campfield, 2009; Floege et al., 1997; Tsujie et al., 2000), and overexpressed during renal disease (Floege, Eitner, & Alpers, 2008; Kirimca, Sarioglu, Camsari, & Kavukcu, 2001; Roy-Chaudhury et al., 1996; Wagrowska-Danilewicz & Danilewicz, 2002). The precise mechanism of tubular loss in our ectopic human kidney grafts remains unknown.

Because the LN provided a supportive niche for the engraftment, vascularization and function of fragments from both mouse (Francipane & Lagasse, 2015, 2016a) and human fetal primary kidney tissues, we next asked whether it could also support functional maturation of isolated or artificially created nephron progenitors (NPs). Reciprocal interactions between the ureteric bud and the metanephric mesenchyme drive kidney development. The metanephric mesenchyme comprises self-renewing, multipotent NPs, which can be identified by their expression of the transcriptional regulator Sine Oculis Homeobox Homolog 2 (SIX2; Kobayashi et al., 2008).

Embryonic kidney single-cell suspensions failed to properly differentiate in the LN, even though they were comprised of SIX2+ cells (Francipane & Lagasse, 2015). When we cotransplanted SIX2+ cells and mouse embryonic kidney fragments (to act as a scaffold and inducer for SIX2+ cells) into the LN, few progenitor cells incorporated into the engrafted

renal tissues and they were unable to mature into meaningful structures (Figures 2a and 2b). We hypothesized that NPs must be grown as organoids and partially differentiated before transplantation for efficient kidney organogenesis in vivo. Overall, this experiment provided a further indication of the potential use of the LN as an in vivo system to monitor the fate of candidate progenitor cell populations.

Recently, substantial advances have been made in the differentiation of NPs—either isolated from embryonic kidneys or obtained from human-induced pluripotent stem cells (hiPSCs)—into cells of kidney lineage. Following culture of NPs into tridimensional aggregates by means of defined media supplemented with recombinant growth factors and low-attachment plates, differentiation can be triggered by exogenous Wnt agonist treatment. Exposure to CHIR99021 (a glycogen synthase kinase-3 inhibitor) results in immediate exhaustion of the progenitors and allows the cells to self-pattern into continuous structures that resemble a nephron (Lam et al., 2014; Li et al., 2016; Morizane et al., 2015; Taguchi & Nishinakamura, 2017; Takasato et al., 2015). Morphological changes are easily observed with a microscope (in the form of condensed structures) and can be thoroughly investigated through whole-mount staining. Markers of mature nephron components (podocytes, proximal tubules, loops of Henle, and distal tubules) and collecting ducts, all indicative of differentiation, are detected (Lam et al., 2014; Li et al., 2016; Morizane et al., 2015; Taguchi & Nishinakamura, 2017; Takasato et al., 2015). By modulating both CHIR99021 exposure times and concentration, it can be possible to obtain a kidney organoid in which specific kidney structures prevail over others. A 3-day CHIR99021 pulse before FGF9 switch in kidney organoids derived from hiPSCs gives rise to more collecting ducts than nephrons, and delaying the timing of FGF exposure by 24 hr leads to the opposite outcome (Takasato et al., 2015). A 2-day pulse with CHIR99021 and FGF2 is sufficient to induce nephrogenesis of mouse NPs (Li et al., 2016). Interestingly, low CHIR99021 concentrations (up to 3 μM) in NP-derived aggregates lead to more glomeruli and less distal tubules, and higher concentrations (around 6 μM) have opposite effects (Li et al., 2016). For in vivo transplantation, 2- to 3-day priming with 4.5 μM CHIR99021 is appropriate to enable subsequent host-derived vascularization of the partially differentiated organoid and thus ensure cell survival and further maturation in the new environment (Li et al., 2016).

SIX2+ mouse NPs produced spherical aggregates when seeded onto 96-well U-bottom low-attachment well plates in NPSR medium (Li et al., 2016) and displayed a robust and homogeneous expression of NP markers (Figure 2c). Aggregates were transplanted in the LN following a short 3-day pulse of 4.5 μM CHIR99021 (27-H76. Reagents Direct). For LN transplantations, exposed LNs were longitudinally cut and a whole organoid was placed between the two LN pieces. One week after transplantation, we observed E-cadherin (CDH1)-/LTL+ and CDH1+/DBA+ tubular structures, indicating in vivo maturation of mouse NPs into proximal and distal tubules, respectively (Figure 2d). Moreover, the grafts contained several host CD31+ ECs, often in contact with WT-1+ aggregates (potential primitive glomeruli; Figure 2d); this shows the feasibility of obtaining vascularized glomerular-like structures from mouse NP-derived kidney organoids in the LN. Later time points did not result in more differentiated structures (data not shown). This result is most likely attributed to the organoid culture, the stability of which after transplantation is yet to

be improved. Aggregates primed with CHIR in vitro likely need additional signals in vivo to complete their functional maturation.

In parallel, we evaluated the behavior of hiPSC-derived kidney organoids inside the LN to broaden LN's utility in the realm of tissue modeling. The WTC-11 hiPSC line was used to generate human kidney organoids. At the start of the experiment, WTC-11 cells were karyotyped, and expression of traditional pluripotency markers was quantified by real-time reverse transcription-polymerase chain reaction (data not shown). We used the protocol developed by the Little laboratory for hiPSC differentiation (Figure 2e1 and e2; Takasato et al., 2015). This protocol allows the generation of organoids containing derivatives of all major renal progenitors, including patterned and segmented nephrons, collecting ducts, renal interstitium, and endothelium. However, nephrons within these organoids are not fully differentiated and lack functioning vasculature. Transplanted organoids in the LN engrafted and showed signs of host EC infiltration in one week (Figure 2e3). A few mouse CD31+ cells localized within WT-1+ aggregates (Figure 2e4). Several LTL+ tubules were also observed (Figure 2e5). Although LTL was present prior to transplantation (Figure 2e1 and e2), there was no CD31 or WT-1 expression in vitro. Importantly, 6 weeks after transplantation we could detect glomerular-like structures containing mouse ECs (CD31 staining) and mature podocytes (PDPLN, Synaptopodin, and PODXL staining) adjacent to presumptive proximal tubules (LTL and Megalin staining; Figure 2e6 and e7). A known byproduct of hiPSC differentiation is the formation of cartilage, which was often observed (data not shown). Thus, although further work must be done before mouse NPs and hiPSC-derived cultures can reproducibly recapitulate adult renal physiology in vivo, our novel organogenesis assay exploiting the use of the LN might help understand how emerging protocols can get closer to obtaining a satisfactory degree of organoid differentiation/function, while reducing the risks of unwanted tissue formation.

In summary, the LN has a unique ability to act as a bioreactor, allowing for substantial expansion of white blood cells during various conditions. This property is exploited by cancer cells, which often transit via the LN where they efficiently grow before disseminating to distant organs. Our group has used this growth-permissive environment to support engraftment and function-testing of fetal mouse kidney, fetal human kidney, and isolated and lab-created NPs. Following early kidney rudiment transplantation, robust kidney tissue forms in which nephron-like structures can be identified by molecular markers. We observed that host vasculature connects to the engrafted tissue allowing host blood to flow through glomeruli, strongly suggesting physiological function of the developing nephrons. Notable features of this engraftment technology make it a unique tool in which to study the organogenetic potential of pluripotent stem cell-derived kidney tissues, as suggested by early engraftment and vascularization of NPs and hiPSCs that were directed toward a renal fate in vitro. Thus, we propose the LN technology as a next-generation platform for testing of de novo generated kidney tissue by colleagues in the field and for disease modeling, drug screening, or translational studies.

Supplementary Material

Refer to Web version on PubMed Central for supplementary material.

ACKNOWLEDGEMENTS

This work was supported by Ri.MED Foundation (M. G. F.), NIH grant R01 DK085711 (E. L.), The Pediatric Device Initiative–McGowan Institute for Regenerative Medicine, University of Pittsburgh–Commonwealth of Pennsylvania SAP4100073573 (E. L., M. G. F., and S. S. L.) and NIH grant R24 DK106743 (L. O.). We thank Lynda Guzik at the McGowan Institute Flow Cytometry Facility for proofreading the manuscript.

Funding information

Pediatric Device Initiative–McGowan Institute for Regenerative Medicine, University of Pittsburgh–Commonwealth of Pennsylvania, Grant/Award Number: SAP4100073573; NIH, Grant/Award Numbers: R01 DK085711 and R24 DK106743; Ri.MED Foundation

REFERENCES

Bariety J, Mandet C, Hill GS, & Bruneval P. (2006). Parietal podocytes in normal human glomeruli. Journal of the American Society of Nephrology, 17(10), 2770–2780. 10.1681/ASN.2006040325 [PubMed: 16943305]

Crisi GM, Marconi SA, Rockwell GF, Braden GL, & Campfield TJ (2009). Immuno-localization of CD44 and osteopontin in developing human kidney. Pediatric Research, 65(1), 79–84. 10.1203/PDR.0b013e31818912b7 [PubMed: 18787423]

Floege J, Eitner F, & Alpers CE (2008). A new look at platelet-derived growth factor in renal disease. Journal of the American Society of Nephrology, 19(1), 12–23. 10.1681/ASN.2007050532 [PubMed: 18077793]

Floege J, Hudkins KL, Seifert RA, Francki A, Bowen-Pope DF, & Alpers CE (1997). Localization of PDGF alpha-receptor in the developing and mature human kidney. Kidney International, 51(4), 1140–1150. 10.1038/ki.1997.157 [PubMed: 9083280]

Francipane MG, & Lagasse E. (2014). Maturation of embryonic tissues in a lymph node: A new approach for bioengineering complex organs. Organogenesis, 10, 323–331. 10.1080/15476278.2014.995509 [PubMed: 25531035]

Francipane MG, & Lagasse E. (2015). The lymph node as a new site for kidney organogenesis. Stem Cells Translational Medicine, 4(3), 295–307. 10.5966/sctm.2014-0208 [PubMed: 25646529]

Francipane MG, & Lagasse E. (2016a). Regenerating a kidney in a lymph node. Pediatric Nephrology, 31(10), 1553–1560. 10.1007/s00467-015-3296-y [PubMed: 26686504]

Francipane MG, & Lagasse E. (2016b). Towards organs on demand: Breakthroughs and challenges in models of organogenesis. Current Pathobiology Reports, 4(3), 77–85. [PubMed: 28979828]

Freedman BS, Brooks CR, Lam AQ, Fu H, Morizane R, Agrawal V, … Bonventre JV (2015). Modelling kidney disease with CRISPR-mutant kidney organoids derived from human pluripotent epiblast spheroids. Nature Communications, 6, 8715 10.1038/ncomms9715

Greenwald AC, Licht T, Kumar S, Oladipupo SS, Iyer S, Grunewald M, & Keshet E. (2019). VEGF expands erythropoiesis via hypoxia-independent induction of erythropoietin in noncanonical perivascular stromal cells. The Journal of Experimental Medicine, 216(1), 215–230. 10.1084/jem.20180752 [PubMed: 30545903]

Grobstein C, & Dalton AJ (1957). Kidney tubule induction in mouse metanephrogenic mesenchyme without cytoplasmic contact. The Journal of Experimental Zoology, 135(1), 57–73. 10.1002/jez.1401350106 [PubMed: 13481289]

Hariharan K, Kurtz A, & Schmidt-Ott KM (2015). Assembling kidney tissues from cells: The long road from organoids to organs. Frontiers in Cell and Development Biology, 3, 70 10.3389/fcell.2015.00070

Kirimca F, Sarioglu S, Camsari T, & Kavukcu S. (2001). Expression of CD44 and major histocompatibility complex class II antigens correlate with renal scarring in primary and systemic renal diseases. Scandinavian Journal of Urology and Nephrology, 35(6), 509–514. [PubMed: 11848433]

Kobayashi A, Valerius MT, Mugford JW, Carroll TJ, Self M, Oliver G, & McMahon AP (2008). Six2 defines and regulates a multipotent self-renewing nephron progenitor population throughout

mammalian kidney development. Cell Stem Cell, 3(2), 169–181. 10.1016/j.stem.2008.05.020 [PubMed: 18682239]

Komori J, Boone L, DeWard A, Hoppo T, & Lagasse E. (2012). The mouse lymph node as an ectopic transplantation site for multiple tissues. Nature Biotechnology, 30(10), 976–983. 10.1038/nbt.2379

Kreidberg JA (2010). WT1 and kidney progenitor cells. Organogenesis, 6(2), 61–70. 10.4161/org.6.2.11928 [PubMed: 20885852]

Lacombe C, Da Silva JL, Bruneval P, Fournier JG, Wendling F, Casadevall N, … Tambourin P. (1988). Peritubular cells are the site of erythropoietin synthesis in the murine hypoxic kidney. The Journal of Clinical Investigation, 81(2), 620–623. 10.1172/JCI113363 [PubMed: 3339134]

Lam AQ, Freedman BS, Morizane R, Lerou PH, Valerius MT, & Bonventre JV (2014). Rapid and efficient differentiation of human pluripotent stem cells into intermediate mesoderm that forms tubules expressing kidney proximal tubular markers. Journal of the American Society of Nephrology, 25(6), 1211–1225. 10.1681/ASN.2013080831 [PubMed: 24357672]

Li Z, Araoka T, Wu J, Liao HK, Li M, Lazo M, … Izpisua Belmonte JC (2016). 3D culture supports long-term expansion of mouse and human nephrogenic progenitors. Cell Stem Cell, 19(4), 516–529. 10.1016/j.stem.2016.07.016 [PubMed: 27570066]

Morizane R, Lam AQ, Freedman BS, Kishi S, Valerius MT, & Bonventre JV (2015). Nephron organoids derived from human pluripotent stem cells model kidney development and injury. Nature Biotechnology, 33(11), 1193–1200. 10.1038/nbt.3392

Nagai T, Yasuoka Y, Izumi Y, Horikawa K, Kimura M, Nakayama Y, … Nonoguchi H. (2014). Reevaluation of erythropoietin production by the nephron. Biochemical and Biophysical Research Communications, 449(2), 222–228. 10.1016/j.bbrc.2014.05.014 [PubMed: 24832733]

Nielsen S, Maunsbach AB, Ecelbarger CA, & Knepper MA (1998). Ultrastructural localization of Na-K-2Cl cotransporter in thick ascending limb and macula densa of rat kidney. The American Journal of Physiology, 275(6 Pt 2), F885–F893. [PubMed: 9843905]

Pan X, Suzuki N, Hirano I, Yamazaki S, Minegishi N, & Yamamoto M. (2011). Isolation and characterization of renal erythropoietin-producing cells from genetically produced anemia mice. PLoS ONE, 6(10), e25839. 10.1371/journal.pone.0025839

Roy-Chaudhury P, Khong TF, Williams JH, Haites NE, Wu B, Simpson JG, & Power DA (1996). CD44 in glomerulonephritis: Expression in human renal biopsies, the Thy 1.1 model, and by cultured mesangial cells. Kidney International, 50(1), 272–281. 10.1038/ki.1996.312 [PubMed: 8807598]

Rygaard J, & Povlsen CO (1969). Heterotransplantation of a human malignant tumour to “Nude” mice. Acta Pathologica et Microbiologica Scandinavica, 77(4), 758–760. [PubMed: 5383844]

Sakata N, Yoshimatsu G, & Kodama S. (2018). The spleen as an optimal site for islet transplantation and a source of mesenchymal stem cells. International Journal of Molecular Sciences, 19(5). 10.3390/ijms19051391

Short KM, Combes AN, Lefevre J, Ju AL, Georgas KM, Lamberton T, … Little MH (2014). Global quantification of tissue dynamics in the developing mouse kidney. Developmental Cell, 29(2), 188–202. 10.1016/j.devcel.2014.02.017 [PubMed: 24780737]

Taguchi A, Kaku Y, Ohmori T, Sharmin S, Ogawa M, Sasaki H, & Nishinakamura R. (2014). Redefining the in vivo origin of metanephric nephron progenitors enables generation of complex kidney structures from pluripotent stem cells. Cell Stem Cell, 14(1), 53–67. 10.1016/j.stem.2013.11.010 [PubMed: 24332837]

Taguchi A, & Nishinakamura R. (2017). Higher-order kidney organogenesis from pluripotent stem cells. Cell Stem Cell, 21(6), 730–746 e736. 10.1016/j.stem.2017.10.011

Takasato M, Er PX, Chiu HS, Maier B, Baillie GJ, Ferguson C, … Little MH (2015). Kidney organoids from human iPS cells contain multiple lineages and model human nephrogenesis. Nature, 526(7574), 564–568. 10.1038/nature15695 [PubMed: 26444236]

Tsujie M, Isaka Y, Ando Y, Akagi Y, Kaneda Y, Ueda N, … Hori M. (2000). Gene transfer targeting interstitial fibroblasts by the artificial viral envelope-type hemagglutinating virus of Japan liposome method. Kidney International, 57(5), 1973–1980. 10.1046/j.1523-1755.2000.00047.x [PubMed: 10792616]

van den Berg CW, Ritsma L, Avramut MC, Wiersma LE, van den Berg BM, Leuning DG, … Rabelink TJ (2018). Renal subcapsular transplantation of PSC-derived kidney organoids induces neo-vasculogenesis and significant glomerular and tubular maturation in vivo. Stem Cell Reports, 10(3), 751–765. 10.1016/j.stemcr.2018.01.041 [PubMed: 29503086]

Wagrowska-Danilewicz M, & Danilewicz M. (2002). A correlation between immunoexpression of CD44, alpha-SMA and CD68+ cells in IgA-nephropathy and in mesangial proliferative IgA-negative glomerulonephritis. Polish Journal of Pathology, 53(3), 155–162. [PubMed: 12476618]

Xu H, Jiao Y, Qin S, Zhao W, Chu Q, & Wu K. (2018). Organoid technology in disease modelling, drug development, personalized treatment and regeneration medicine. Experimental Hematology & Oncology, 7, 30 10.1186/s40164-018-0122-9

Zehnder D, Bland R, Walker EA, Bradwell AR, Howie AJ, Hewison M, & Stewart PM (1999). Expression of 25-hydroxyvitamin D31alpha-hydroxylase in the human kidney. Journal of the American Society of Nephrology, 10(12), 2465–2473. [PubMed: 10589683]

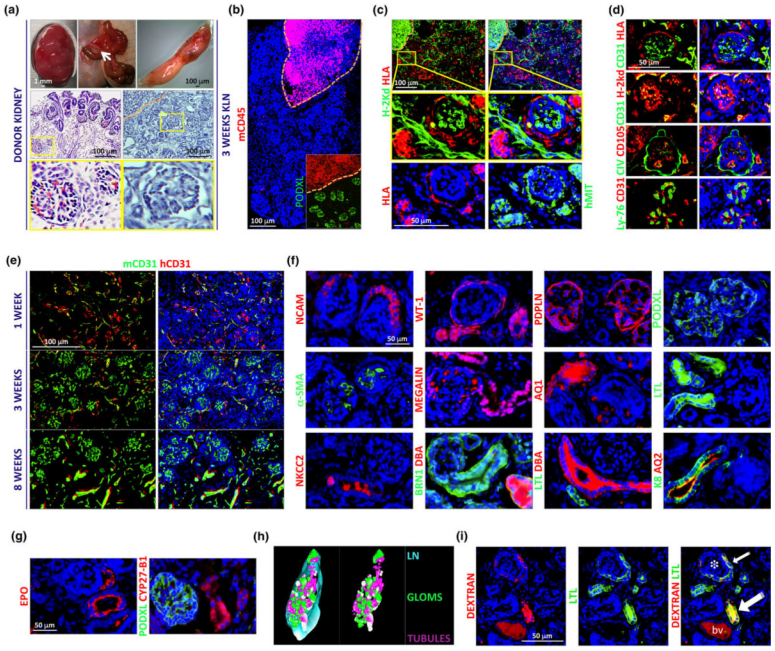

FIGURE 1.

The mouse lymph node (LN) supports engraftment, vascularization, and function of human fetal kidneys. (a) Top panels, from left to right: images of human fetal kidney, mesenteric area of a recipient BALB/c nude mouse containing jejunal LNs (arrow), and isolated LNs 3 weeks after kidney transplantation. Middle panels, left: representative hematoxylin and eosin staining of donor human fetal kidney paraffin section. Middle panel, right: representative hematoxylin staining of LN frozen section 3 weeks after kidney transplantation. The region enclosed by the orange dashed line in the upper left corner indicates non-engrafted LN's area. Bottom panels: the insets show a nonmature (left) or a mature (right) glomerulus. (b) Representative immunofluorescence staining of a 3-week graft frozen section for mouse CD45 (red) and human Podocalyxin (PODXL, green). Nonengrafted LN's area (red) is enclosed by an orange dashed line. (c) Representative immunofluorescence staining of 3-week graft frozen sections for BALB/c nude mouse H-2kd (green) + human leukocyte antigen (HLA, red), or human mitochondria (hMIT, green). Nonengrafted LN's area is enclosed by an orange dashed line in the top left corners. Enlarged views of the boxed regions are shown. (d) Representative immunofluorescence staining of 3-week graft frozen sections for human/mouse CD31 (green) + HLA (red), human/mouse CD31 (green) + H-2kd (red), human/mouse Collagen IV (CIV, green) + human/mouse CD105 (red), or mouse Ly-76 (green) + human/mouse CD31 (red). (e) Representative immunofluorescence staining of 1−, 3− and 8-week graft frozen sections for mouse (green) and human (red) CD31. Images show progressive replacement of donor endothelial cells with host endothelial cells. (f) Representative immunofluorescence staining of 3-week graft frozen sections for human neural cell adhesion molecule (red), human/mouse Wilms' Tumor 1 (WT-1, red), human/mouse Podoplanin (PDPLN, red), human PODXL (green), human/mouse Alpha-smooth muscle actin (α-SMA, green), human/mouse Megalin (red), human/mouse Aquaporin 1 (AQ1, red), human/mouse Lotus tetragonolobus lectin (LTL, green), human/mouse Sodium-Potassium-Chloride Cotransporter 2 (NKCC2, red), human BRN1 (green) + human/mouse

Dolichos biflorus agglutinin (DBA, red), human/mouse LTL (green) + human/mouse DBA (red), or human/ mouse Cytokeratin-8 (K8, green) + human/mouse Aquaporin 2 (AQ2, red). (g) Representative immunofluorescence staining of 3-week graft frozen sections for human/ mouse Erythropoietin (EPO, red) or human/mouse Cytochrome P450 Family 27 Subfamily B Member 1 (CYP27-B1, red) + human PODXL (green). (h) Representative 3D reconstruction of an 8-week graft. Layers from serial hematoxylin and eosin-stained LN sections were generated by tracing the engrafted LN margin, glomeruli and tubules. Traced layers were then aligned, and 3D images of the engrafted tissues were rendered. Left panel: image of engrafted glomeruli (green or white) and tubules (purple) inside the LN (light blue). Right panel: image with glomeruli and tubules only. (i) Tubular functions in human kidney grafts were assessed by injecting recipient mice IP with 200μl of 5mg/ml lysine-fixable Texas Red 10,000 MW Dextran 2 hours before sacrifice. The image shows Dextran accumulation (red) in a glomerular-like structure (*) near the LTL+ urinary pole (green, small arrow), and in an LTL+ proximal tubule (green, big arrow) of an 11-week kidney graft. Bv = blood vessel. Nuclei were counterstained using Hoechst (blue)

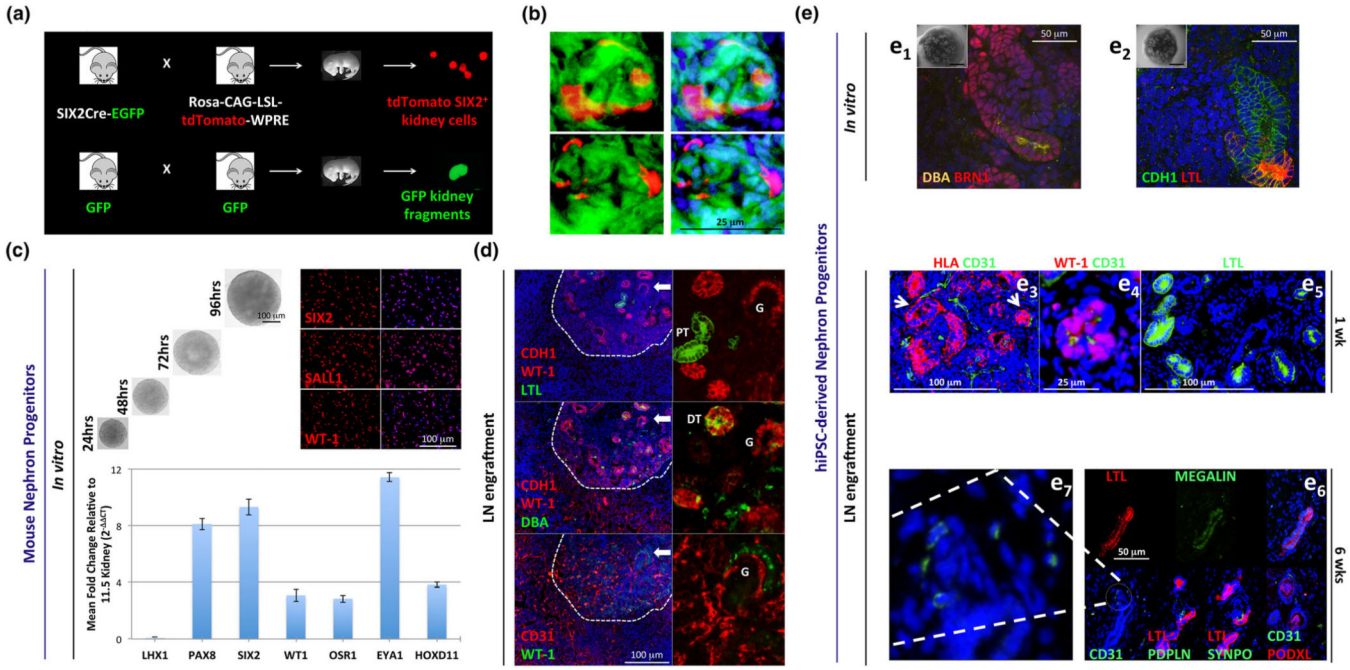

FIGURE 2.

Lymph node (LN) engraftment of mouse kidney nephron progenitor (NP) single-cell suspensions and organoid cultures derived from freshly-isolated mouse NPs or human induced pluripotent stem cells (hiPSCs). (a) Schematic representation of transgenic mouse breeding. Embryonic kidneys were retrieved from embryos generated through crossing SIX2-Cre-EGFP mice with Rosa-CAG-LSL-tdTomato-WPRE mice. The purpose of this cross was to create a SIX2 population permanently labeled with tdTomato. tdTomato+ cells were purified via Fluorescence-activated cell sorting (FACS), mixed with GFP+ mouse embryonic kidney fragments, and transplanted into jejunal LNs. (b) Serial frozen sections of a representative glomerulus with the presence of SIX2-derived cells 5 weeks after LN transplantation. (c) Top panel, left: time-lapse bright-field images showing the morphology/size of live mouse NP aggregates growing in NPSR medium. Top panel, right: expression of NP markers in disaggregated cells, as assessed by immunofluorescence analysis. Bottom: real-time reverse transcription-polymerase chain reaction analysis in NP aggregates for different markers, with respect to an E11.5 kidney. *GAPDH* was used to normalize gene expression data. Relative changes in gene expression were calculated using the $2^{-\Delta\Delta CT}$ method and were presented as mean ± SD. All primer sequences were retrieved from Li et al., 2016. (d) Representative immunofluorescence staining of 1-week organoid graft frozen sections for human E-cadherin (CDH1, red) + WT-1 (red) + LTL (green), CDH1 (red) + WT-1 (red) + DBA (green), or CD31 (red) + WT-1 (green). PT= proximal tubule; DT= distal tubule; G=glomerulus. (e1 and e2). Representative confocal fluorescent images of hiPSC-derived kidney organoids stained for DBA (orange) + BRN1 (red) or CDH1 (green) + LTL (red) before transplantation. Insets with images of stained organoids are provided at the top left corners. (e3) HLA (red) + mouse CD31 (green) costaining reveals host vessels near a potential glomerulus and tubule (left and right arrows, respectively) 1 week after organoid transplantation into the LN. (e4) Human/mouse WT-1 (red) + mouse CD31 (green)

costaining confirms endothelial cell (EC) infiltration in a potential primitive glomerulus. (e5) Human/mouse LTL staining (green) indicates the presence of several potential proximal tubules in the engrafted tissue. (e6) Serial frozen sections showing a nephron-like structure comprised by presumptive proximal tubule reactive to human/mouse LTL (red) + human/mouse Megalin (green) and connected to a glomerular-like area containing mouse CD31+ (green) ECs and presumptive podocytes (mouse/human Podoplanin, mouse/human SYNPO, human PODXL), 6 weeks after organoid transplantation into the LN. Infiltrating mouse ECs in the glomerular-like area are shown at higher power in e7. Nuclei were counterstained using Hoechst (blue)